CHAPTER 1

Introduction

1.1 THE SUBJECT

Accelerators are devices that control and manipulate the motion of charged particles. To design an accelerator, one starts by considering the motion of a single particle. To describe the dynamics of a beam of particles, one then regards the beam as a collection of noninteracting single particles moving in the environment prescribed by the accelerator design. The environment is defined by the electric and magnetic fields of the various accelerator components specified in the design. Given these fields, intricate effects of linear and nonlinear dynamics of a single particle can be studied in detail.

Many accelerator applications, however, require beams of medium or high intensities. As the beam intensity is increased, the electromagnetic fields self-generated by the beam, particularly the fields generated by the beam interacting with its immediate surroundings, will perturb the external prescribed fields. When the perturbation becomes sufficiently strong, the beam becomes unstable. To describe this aspect of the beam dynamics, the single-particle picture does not suffice and a multiparticle picture is introduced. This multiparticle picture takes into consideration the important self-generated fields, but usually omits the detailed nonlinear aspects included in the single-particle picture.

To be more specific, consider an intense particle beam contained in a metallic vacuum chamber of an accelerator. The beam interacts electromagnetically with its surroundings to generate an electromagnetic field, known as the *wake field*. This field then acts back on the beam, perturbing its motion. Under unfavorable conditions, the perturbation on the beam further enhances the wake field; the beam-surroundings interaction then leads to an instability, known as a *collective instability*, and a subsequent beam loss. The beam and its surroundings form a self-consistent dynamical system, and it is this system that we will study. Thus,

$$\begin{aligned} \text{dynamical system} &= \text{beam} + \text{surroundings}, \\ \text{mediator of interaction} &= \text{wake field}. \end{aligned} \tag{1.1}$$

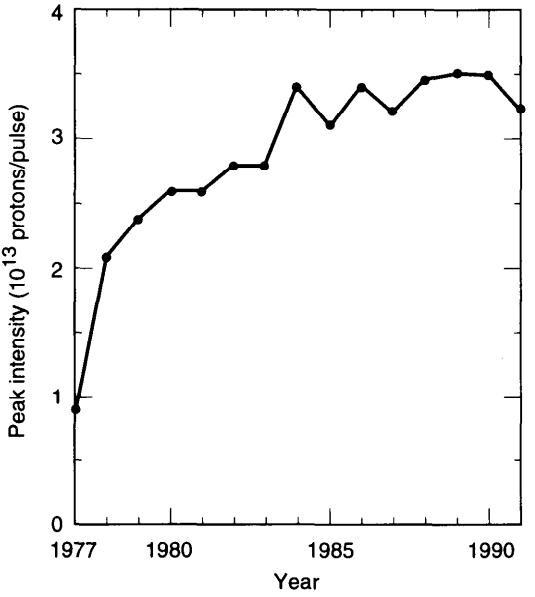

Figure 1.1. Peak beam intensity of the CERN Super Proton Synchrotron from 1977 to 1991. (Courtesy Jacques Gareyte, 1991.)

The subject of collective instabilities in high energy accelerators has been studied since the late 1950s and early 1960s. The importance of the subject lies in the fact that it is one of the main factors that determine the ultimate performance of the accelerator. The advancement of this subject over the years can be evidenced by the discovery and curing of several collective instability mechanisms. Each accelerator, when pushed for performance, will encounter some intensity limit. After this limit is analyzed, understood, and possibly cured, a new limit emerges. The process repeats, and the end result is the improved understanding and higher performance of the accelerator. One example is illustrated in Figure 1.1, the record of the peak beam intensity reached at the CERN Super Proton Synchrotron over the years. The confidence gained in turn provides a basis for ever more daring proposals for new accelerators.[1] Today, the subject has grown into a large collection of activities.[2] Each activity constitutes an important research area; each

[1]One can come up with an impressive list here: linear colliders, high luminosity circular colliders, free electron laser drivers, modern synchrotron light sources, inertial fusion drivers, etc.

[2]Another impressive list is in order: methods to measure the impedance, beam diagnostic techniques, beam cooling techniques, numerical simulation methods, calculation of wake fields and impedances of complex objects, impedance budgeting in accelerator design, feedback systems, and various theoretical studies.

needs to be understood or implemented on the accelerators of the future. In comparison, the present volume is merely one attempt to introduce the subject, and only some of the above-mentioned activities will be covered in detail.

In the rest of Chapter 1, we will first describe the simplified accelerator model upon which our investigations will be built. The *space charge effect*, the most basic collective phenomenon, will then be discussed in detail; these discussions provide a background for later developments.

In Chapter 2, the Maxwell equations are solved to obtain the wake field of a beam with a rigid particle distribution. The action of the wake field on the particle distribution is neglected here; thus the beam-surroundings system is not solved self-consistently. The concepts of *wake function* and *impedance* will be introduced and their properties investigated. As an illustration, the special case of a vacuum chamber pipe with a resistive wall will be presented explicitly. The equations needed in Chapters 1 and 2 are basically the Maxwell equations.

In Chapters 3 and 4, the influence of wake fields on the beam will be studied—Chapter 3 for linear accelerators (linacs), Chapter 4 for circular accelerators. In Chapter 4 and part of Chapter 3, the discussions are carried out with a simplified model for the beam distribution. In fact, the beam will be represented as a point charge without any internal structure. The beam-surroundings system is solved self-consistently with the restriction that the beam is allowed to have only a center-of-mass motion. This simplified view allows a few of the collective instability mechanisms to be studied. These *one-particle models* are sufficiently successful that the treatment is extended to include a few *two-particle models*, in which the beam is represented as two point-macroparticles interacting with each other through the wake forces. This picture gives an insight into the internal motions within the beam. The equation used in Chapters 3 and 4 is basically $F = ma$.

An important topic is treated in Chapter 5, namely, *Landau damping*. Since our preference is to postpone formal treatments until later, Chapter 5 attempts to describe the Landau damping mechanism using a direct treatment instead of the more conventional Vlasov technique.

A self-consistent treatment of the beam-surroundings system that permits a full evaluation of the internal beam motions will be given in Chapter 6. Here the equation of motion—the *Vlasov equation*—is established to describe the system. The formalism that allows the solution of this equation will then be presented. Results obtained in the previous chapters, as well as some additional results, will be derived or rederived.[3]

[3]Depending on choice of emphasis, some material may be skipped. One possible choice of emphasis would skip, for example, Sections 1.4, 1.5, 1.6, 2.4, 3.3, 4.4, 5.2, 6.8, and 6.9.

We will use cgs units. To convert to other unit systems, it is convenient to apply the following conversions:

$$\frac{4\pi}{c} = Z_0 = \text{impedance of free space} = 120\pi\ \Omega \approx 377\ \Omega, \quad (1.2)$$

$$\frac{e^2}{m_0 c^2} = r_0 = \text{classical radius of the particle}$$

$$= \begin{cases} 2.818 \times 10^{-13}\ \text{cm} & \text{for electrons,} \\ 1.535 \times 10^{-16}\ \text{cm} & \text{for protons,} \end{cases} \quad (1.3)$$

where c is the speed of light, and e and m_0 are the electric charge and rest mass of the particle under consideration. Equation (1.2) follows from the conversion $1\ \Omega = 1/30c \approx \frac{1}{9} \times 10^{-11}$ s/cm in the cgs system.

1.2 FREE SPACE AND A PERFECTLY CONDUCTING SMOOTH PIPE

The electromagnetic field carried by a relativistic point charge q in free space is a familiar subject treated in textbooks.[4] The field distribution, shown in Figure 1.2(a), is Lorentz contracted into a thin disk perpendicular to the particle's direction of motion with an angular spread on the order of $1/\gamma$, where γ is the Lorentz energy factor. In the ultrarelativistic limit of $v = c$, the disk shrinks into a δ-function thickness, as shown in Figure 1.2(b). The electric field $\vec{E}$ points strictly radially outward from the point charge. The magnitude of $\vec{E}$ is most easily obtained by drawing a pillbox with radius r and an infinitesimal height around the charge q, as shown in Figure 1.2(b), and then applying Gauss's law.[5] The result is

$$E_r = \frac{2q}{r}\delta(s - ct), \quad (1.4)$$

where we have adopted a cylindrical coordinate system (r, θ, s) with s pointing in the direction of motion of q.[6] Similarly, an application of

[4]See, for example, J. D. Jackson, *Classical Electrodynamics*, 2nd ed., Wiley, New York, 1975.

[5]The reader is reminded of the remarkable fact that Gauss's law is valid even if the charges under consideration are moving with relativistic speeds. The reader should also recall that Lorentz contraction does not cause bending of field lines; the field lines are straight lines pointing radially outward and get bent only when the charge is accelerated.

[6]We use s to designate the absolute longitudinal position in the laboratory frame. The more conventional symbol z is reserved to designate the *relative* longitudinal position of a particle relative to a comoving reference particle.

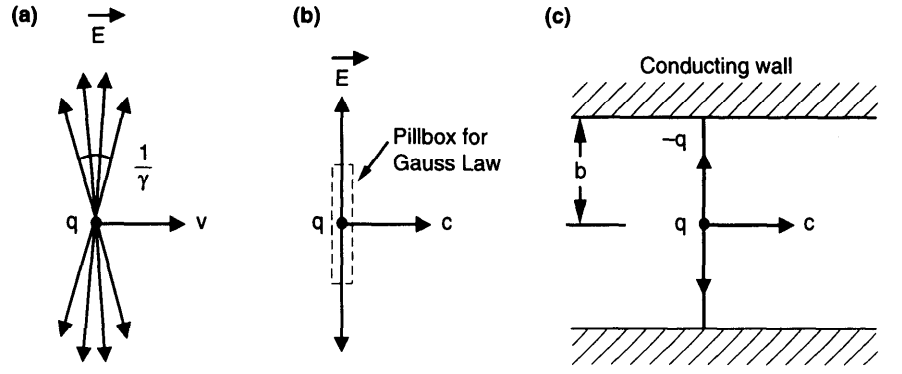

Figure 1.2. Electromagnetic field carried by an ultrarelativistic point charge: (a), (b) in free space; (c) in a perfectly conducting smooth pipe.

Ampere's law gives

$$B_\theta = \frac{2q}{r}\delta(s - ct), \tag{1.5}$$

which is equal to E_r. The shape of the field distribution resembles a pancake moving with the charge.

We now consider the case in which the point charge moves along the axis of an axially symmetric vacuum chamber pipe that is perfectly conducting, as shown in Figure 1.2(c). The same application of Gauss's and Ampere's laws again provides the results (1.4) and (1.5). The sole effect of the pipe wall is to truncate the field lines by terminating them onto the image charges and currents on the wall.

The above result that the pipe simply truncates the field lines without deformation applies only if the charge moves along the pipe axis. It is no longer correct for a point charge moving off-axis. One can consider, for instance, a particle that moves down the pipe with an offset a in the $\theta = 0$ direction. The charge and current density can be decomposed in terms of multipole moments,

$$\rho = \sum_{m=0}^{\infty} \rho_m \quad \text{and} \quad \vec{j} = \sum_{m=0}^{\infty} \vec{j}_m, \tag{1.6}$$

where the distribution with a pure mth moment is given by

$$\begin{aligned} \rho_m &= \frac{I_m}{\pi a^{m+1}(1 + \delta_{m0})}\delta(s - ct)\delta(r - a)\cos m\theta, \\ \vec{j}_m &= c\rho_m \hat{s}, \end{aligned} \tag{1.7}$$

where $\delta_{m0} = 1$ if $m = 0$, 0 if $m \neq 0$. In Eq. (1.7), the charge is distributed as an infinitesimally thin ring with radius a and with a $\cos m\theta$ angular dependence. The quantity I_m is the mth moment of the beam. The monopole moment I_0 is simply the net charge q of the beam. For an offset point charge, $I_m = qa^m$.

The reason that the pipe no longer simply truncates the free space field lines in this case is that if a simple truncation is made, the boundary conditions are no longer fulfilled, because the electric field is no longer perpendicular, and the magnetic field is no longer parallel, to the pipe wall. Indeed, the electromagnetic field carried by the $\cos m\theta$ ring beam (1.7) is obtained by solving the Maxwell equations together with proper boundary conditions. The result is

$$
\begin{aligned}
E_r &= \frac{2I_m}{1+\delta_{m0}}\delta(s-ct)\cos m\theta \begin{cases} \left(\frac{1}{b^{2m}} - \frac{1}{a^{2m}}\right) r^{m-1}, & r < a, \\ \frac{1}{r^{m+1}} + \frac{r^{m-1}}{b^{2m}}, & a < r < b, \end{cases} \\
E_\theta &= \frac{2I_m}{1+\delta_{m0}}\delta(s-ct)\sin m\theta \begin{cases} -\left(\frac{1}{b^{2m}} - \frac{1}{a^{2m}}\right) r^{m-1}, & r < a, \\ \frac{1}{r^{m+1}} - \frac{r^{m-1}}{b^{2m}}, & a < r < b, \end{cases} \\
B_r &= -E_\theta, \\
B_\theta &= E_r.
\end{aligned}
\tag{1.8}
$$

The derivation of Eq. (1.8) is omitted here. It can be reproduced as a special case of what we will derive in Section 2.1. [See discussion following Eq. (2.35).] The important facts here are that the particle has generated a field that has an angular dependence of $\sin m\theta$ and $\cos m\theta$, and that the field is Lorentz contracted into a δ-function in its longitudinal distribution. No wake field is left behind the particle as a result of this beam-environment interaction. The fact that a $\cos m\theta$ beam generates a field that has only the $\cos m\theta$ and $\sin m\theta$ angular dependences means different multipoles are decoupled, and is a consequence of the axial symmetry assumed.

Figure 1.3 shows the electric field pattern in the "pancake region" $s = ct$. Note that the electric field is perpendicular to the boundary $r = b$, but is not perpendicular to $r = a$ where the ring beam is located. Also, the field is not continuous across $r = a$.

There is no field inside the ring beam ($r < a$) for $m = 0$. The field pattern is uniform inside the beam for $m = 1$, and resembles the field inside a dipole magnet. Similarly, for $m = 2$ the field pattern resembles that of a quadrupole magnet, and for $m = 3$ a sextupole magnet.

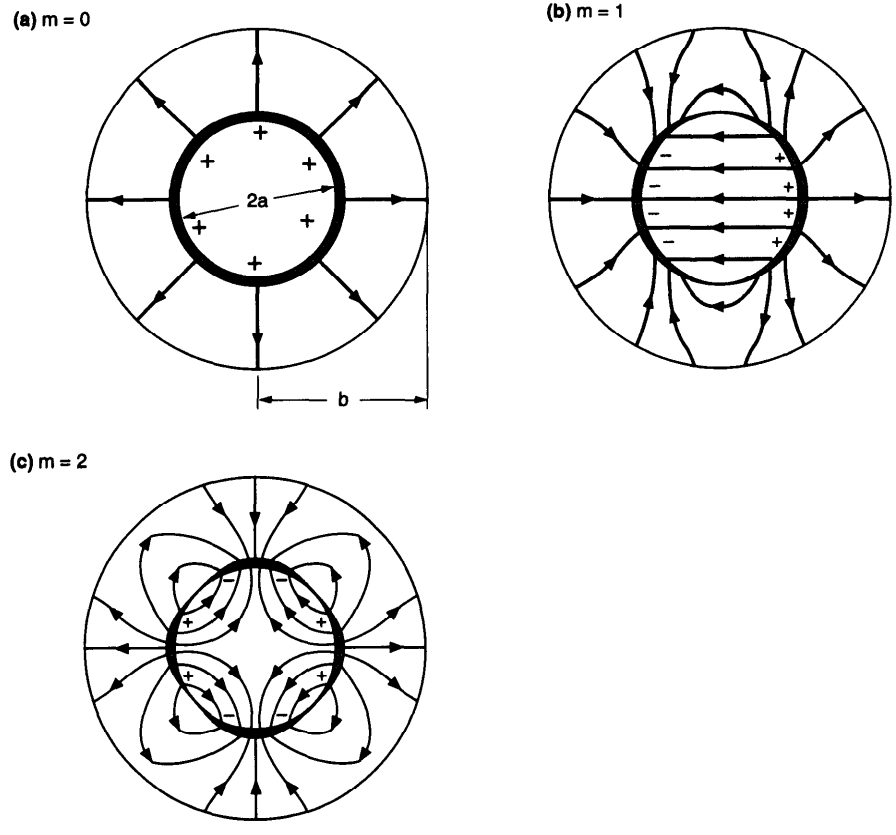

Figure 1.3. Electric field pattern associated with a $\cos m\theta$ ring beam. (a), (b), (c) are for $m = 0, 1, 2$, respectively. Shaded regions indicate the beam.

In free space or in a perfectly conducting pipe, because of the $\delta(s - ct)$ dependence in Eq. (1.8), an ultrarelativistic particle does not see the fields carried by other particles in the beam—unless the two particles move side by side with exactly the same longitudinal position, in which case they see each other's fields, but do not experience any Lorentz force because the electric force and the magnetic force cancel exactly.[7] Consequently, there can be no collective instability. Thus we arrive at one important conclusion, namely, for a collective instability to occur, the beam must not be ultrarelativistic, or its environment must not be a perfectly conducting smooth pipe.

[7]It is true that there is an electrostatic force in the rest frame of the beam, but when observed in the laboratory frame, motions are infinitely time dilated.

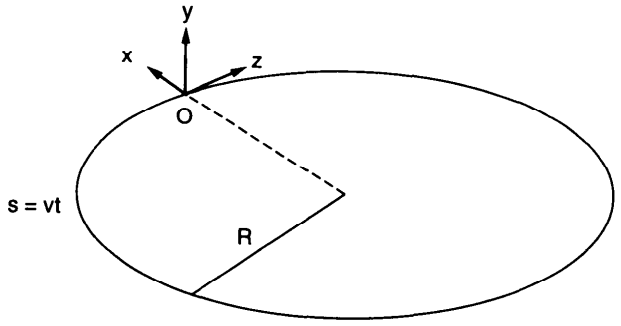

Figure 1.4. The accelerator model. The quantities x, y, and z are the horizontal, vertical and longitudinal coordinates of a particle relative to a reference particle O, which travels along the circumference with $s = vt$. The accelerator has a circumference $2\pi R$.

1.3 THE ACCELERATOR MODEL

We will model a circular accelerator so that its designed beam trajectory is a circle of circumference $2\pi R$. The beam circulates around the circumference inside a metallic vacuum chamber of a varying cross section. The unperturbed single-particle motion will be modeled as simple harmonic oscillators in the horizontal, vertical, and longitudinal coordinates x, y, and z with angular frequencies ω_{x0}, ω_{y0}, ω_{s0}, respectively.[8] We define the tunes $\nu_{x0,\,y0,\,s0}$ to be these frequencies divided by the particle's revolution frequency ω_0. See Figure 1.4. Typically we have $\nu_{x0} \gg 1$, $\nu_{y0} \gg 1$, and $\nu_{s0} \ll 1$.

The reference particle O has exactly the design energy and follows exactly the design orbit turn after turn in the accelerator. This fictitious particle is called the *synchronous* particle. Its trajectory will be designated by a coordinate s, which will have the meaning of the time variable in our description. The motions of all other particles are described relative to the synchronous particle. To completely describe the motion of a particle, we need six coordinates $(x, x', y, y', z, \delta)$ in the six-dimensional phase space, where $x' = dx/ds$ and $y' = dy/ds$ are the slopes of the horizontal and vertical coordinates of the particle relative to the designed direction of motion, and $\delta = \Delta P/P$ is the relative momentum error of the particle. The synchronous particle will have all six coordinates equal to zero. Under these assumptions our accelerator model can be summarized by the following unperturbed

[8]It is not possible to have *simultaneous* focusing in all three dimensions at a given time and space in an accelerator. The strong focusing accelerators, for example, do not provide simultaneous focusing in x and y. However, the job of an accelerator designer is to design an environment for the beam particles that resembles as much as possible a three-dimensional simple harmonic potential well which focuses in all three dimensions, although only in an *average* sense.

equations of motion for single particles:

$$\begin{aligned} x'' &+ \left(\frac{\nu_{x0}}{R}\right)^2 x = 0, \\ y'' &+ \left(\frac{\nu_{y0}}{R}\right)^2 y = 0, \\ z' &= -\eta\delta, \\ \delta' &= \begin{cases} 0, & \text{unbunched beams,} \\ \dfrac{1}{\eta}\left(\dfrac{\nu_{s0}}{R}\right)^2 z, & \text{bunched beams,} \end{cases} \end{aligned} \tag{1.9}$$

where a prime means taking the derivative with respect to s, and η is the *slippage factor* defined as

$$\eta = \alpha - \frac{1}{\gamma^2}, \tag{1.10}$$

with α an accelerator design constant called the *momentum compaction factor* and $\gamma = 1/\sqrt{1 - (v/c)^2}$. In a circular accelerator, α is typically positive and is approximately equal to $1/\nu_{x0}^2$. For high energy applications, $\delta = \Delta P/P$ is approximately equal to the relative energy error $\Delta E/E$.

The first two members in Eq. (1.9) describe the simple harmonic property of the *transverse betatron oscillation* of the particles. For the transverse motion, it is often useful to relate the tunes to the β-functions β_x and β_y of the accelerator design.[9] In the smooth accelerator model presently being considered, $2\pi\beta_{x,y}$ are just the betatron oscillation wavelengths, related to the tunes by

$$\nu_{x0} = \frac{R}{\beta_x} \quad \text{and} \quad \nu_{y0} = \frac{R}{\beta_y}. \tag{1.11}$$

Equation (1.9) also applies to linacs, provided one sets $\alpha = 0$ and replaces $\nu_{x0,y0}/R$ by $1/\beta_{x,y}$.

For ultrarelativistic cases, $\gamma \to \infty$, η is approximately equal to α and is most likely positive. For energies lower than a transition energy corresponding to $\gamma_{tr} \equiv 1/\sqrt{\alpha}$, η becomes negative. The accelerator operation is *below transition* if $\gamma < \gamma_{tr}$ and *above transition* if $\gamma > \gamma_{tr}$. When an accelerator is operated below transition, the longitudinal coordinate z of a particle, whose energy is slightly higher than the design energy ($\delta > 0$), will increase with

[9] E. D. Courant and H. S. Snyder, Ann. Phys. **3**, 1 (1958).

time s (i.e. $z' > 0$). On the other hand, if the accelerator is operated above transition, a higher energy particle will *slow down* ($z' < 0$) even though its actual velocity is higher than that of the synchronous particle. This unexpected sign is called the *negative mass* effect, and is due to the fact that higher energy particles will have to make larger orbits as they circulate around the accelerator. For linacs ($\alpha = 0$) the operation is always below transition.

Combining the two longitudinal equations for z and δ in Eq. (1.9), one obtains the *longitudinal synchrotron oscillation*

$$z'' + \left(\frac{\nu_{s0}}{R}\right)^2 z = 0. \tag{1.12}$$

For unbunched beams, the accelerator is operated with no longitudinal focusing; the equations of motion for z and δ can be described by Eq. (1.12) if we set $\nu_{s0} = 0$, and therefore can be considered a special case of bunched motion. However, we separate the bunched and unbunched cases explicitly because their beam dynamics are quite different.

At transition, $\eta = 0$, the flow of particles in the longitudinal phase space freezes. This is the moment when the beam is most vulnerable to perturbations and is a concern for accelerators (particularly proton synchrotrons) whose operation is such that the beam energy is accelerated to cross transition. Special care is often required to deal with transition crossing.

For an unbunched beam, δ does not change with time, and z' depends on δ. The unperturbed beam has a uniform longitudinal distribution with particles shearing against each other due to a spread in their energies. The particle motion in the three phase spaces (x, x'), (y, y'), and (z, δ) is shown in Figure 1.5. Unless otherwise noted, we ignore coupling among the three degrees of freedom.

Equation (1.9), together with Eqs. (1.10–1.12), describes our accelerator model.[10] They specify the unperturbed motions. Based on this model, one can study the various stability problems by introducing perturbations. Adding nonlinear terms on the right hand side of these equations, for example, leads to the study of single-particle nonlinear dynamics. We will study another type of perturbations, namely those due to collective electromagnetic fields.

[10]To explore the physics of accelerators further, read Henri Bruck, *Accélérateurs Circulaire de Particules*, Univ. France Press, 1966, English transl. LASL Report LA-TR-72-10(R); Matthew Sands, *The Physics of Electron Storage Rings, An Introduction*, SLAC Report 121 (1970); J. D. Lawson, *The Physics of Charged-Particle Beams*, Clarendon Press, Oxford, 1977; Stanley Humphries, Jr., *Principles of Charged Particle Acceleration*, Wiley, New York, 1986; N. S. Dikanski and D. V. Pestrikov, *Physics of Intense Beams in Storage Rings*, Nauka Publishers, Novosibirsk, 1989 (in Russian); Stanley Humphries, Jr., *Charged Particle Beams*, Wiley, New York, 1990; D. A. Edwards and M. J. Syphers, *An Introduction to the Physics of High Energy Accelerators*, Wiley, New York, 1993.

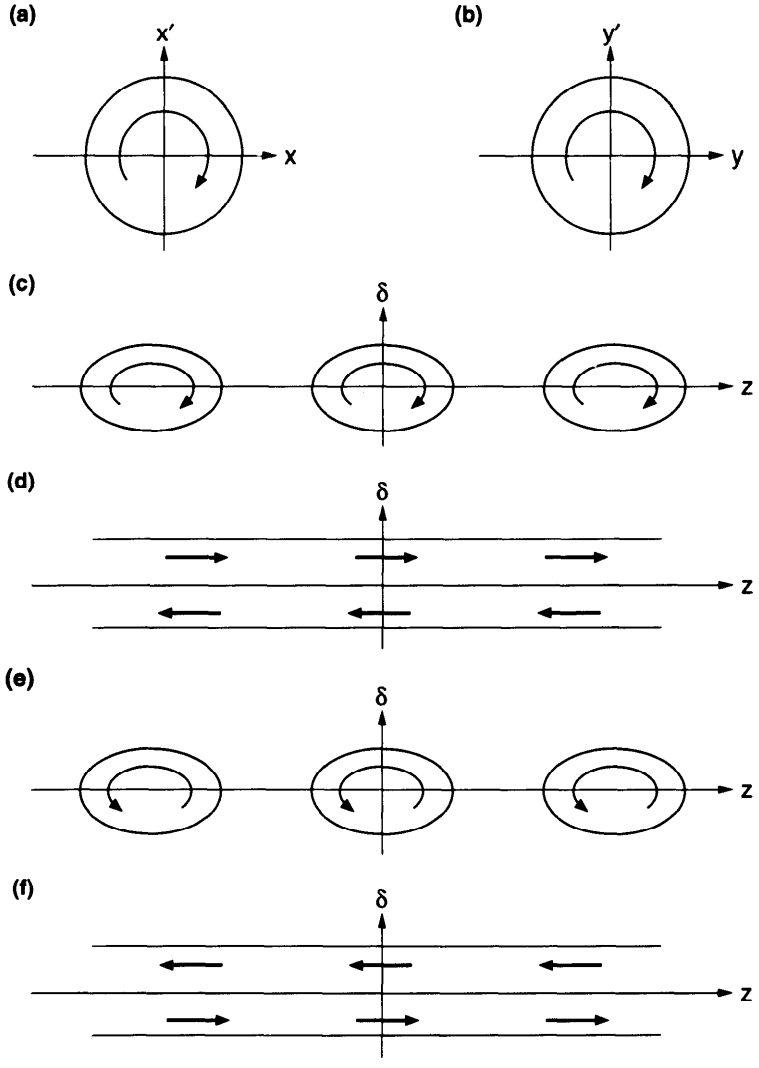

Figure 1.5. Motion of a distribution of particles in phase spaces. Arrows indicate the direction of motion of particle trajectories. (a) and (b) are transverse phase spaces. (c) and (d) are longitudinal phase spaces for bunched and unbunched beams below transition. (e) and (f) are the same as (c) and (d) but above transition. In (c) and (e), the two adjacent bunches are also shown. In the longitudinal phase space, there is a shearing of the particle flow pattern in the unbunched case. Note that the flow direction reverses as beam energy crosses transition. At transition, the flow pattern freezes. Above transition, the rotation is counterclockwise, which is opposite to the transverse cases and is a consequence of the negative mass effect.

Before leaving the subject of accelerator model, it is useful here to introduce the concept of a *tune shift*. Consider the case when the perturbation affects the focusing in y-motion, i.e., the perturbation is linear in y:

$$y'' + \left(\frac{\nu_{y0}}{R}\right)^2 y = Ky. \tag{1.13}$$

The perturbed motion can be described by a perturbed tune ν_y determined by

$$\nu_y^2 = \nu_{y0}^2 - KR^2. \tag{1.14}$$

For small perturbation $|KR^2| \ll \nu_{y0}^2$, the tune has shifted by an amount[11]

$$\Delta\nu_y = \nu_y - \nu_{y0} = -\frac{KR^2}{2\nu_{y0}}. \tag{1.16}$$

In case the linear perturbation (linear in y) occurs at a localized position around the accelerator, the right hand side of Eq. (1.13) reads $Ky\delta_p(s)2\pi R$, where δ_p is the periodic δ-function with period $2\pi R$. The tune shift to the first order in K is still given by Eq. (1.16). This means that, to the first order, the effect of a linear perturbation is the same whether it is spread out over the circumference of the accelerator or lumped at a discrete location. This approximation amounts to ignoring the resonance effects when ν_{y0} is close to half integers.

The concept of tune shift—the simplest manifestation of which is illustrated in Eqs. (1.13–1.16)—plays a crucial role in the study of collective effects. In later chapters, what we will often compute is $\Delta\nu$ when the perturbations are due to collective electromagnetic fields, and in general the tune shift is complex.[12] This point will become clear as the subject develops.

[11]For readers familiar with the formula

$$\Delta\nu = \frac{1}{4\pi}\oint ds\,\beta_y\,\Delta G = \frac{1}{2\pi}\oint ds\,\frac{\beta_y}{2}\,\Delta G, \tag{1.15}$$

the factor $\beta_y/2$ in the expression has the same physical meaning as the factor $1/2\nu_{y0}$ in Eq. (1.16) [see Eq. (1.11)], which in turn has the simple origin of Eq. (1.14), and is not something mysterious.

[12]Two particular aspects are worth mentioning here for later reference. (1) Just as the tune shift is independent of the detailed distribution of gradient errors around the accelerator (away from resonances), the detailed distribution of the impedance (which gives rise to the collective mode frequency shift and growth rate) does not matter and can often be regarded as being uniformly distributed around the accelerator for simplicity. (2) For the transverse collective effects, the mode frequency shifts and growth rates obtained using an uniformly distributed impedance can be modified to yield the result for a localized impedance by simply replacing $R/\nu \to \beta_Z$, where β_Z is the β-function at the location of the impedance.

1.4 TRANSVERSE SPACE CHARGE EFFECTS

The first collective effect to be considered is the space charge effect. It was previously mentioned that there are no collective effects in free space or in a perfectly conducting smooth pipe in the ultrarelativistic limit $\gamma \to \infty$. To study the space charge effect, we back off from this limit, although we will still consider a moderately relativistic beam with $\gamma \gg 1$. One difference between the ultra and moderate relativisticities was illustrated in Figure 1.2(a) and (b). In this and the next sections, we will study the transverse and longitudinal effects of the space charge forces on the motion of particles in the beam.

Consider an unbunched beam that has a longitudinal line charge density λe and moves with speed βc. Let N be the total number of particles in the beam; we have $\lambda = eN/2\pi R$. Let the beam have a round transverse distribution which is uniform up to a radius a. We consider the motion of a test particle in the beam at a radial distance r ($r < a$) away from the beam axis. Applying Gauss's law yields the electric field seen by the particle,

$$E_r = \frac{2\lambda e}{a^2} r. \tag{1.17}$$

Similarly, application of Ampere's law gives

$$B_\theta = \frac{2\lambda e\beta}{a^2} r = \beta E_r. \tag{1.18}$$

The Lorentz force experienced by the particle is in the radial direction,

$$F_r = e(E_r - \beta B_\theta) = \frac{2\lambda e^2}{a^2\gamma^2} r. \tag{1.19}$$

Note that the electric and magnetic forces almost cancel each other, yielding the factor of γ^2 in the denominator. The direct space charge effect is therefore nonrelativistic in nature.

Consider the vertical motion of the particle. The equation of motion is

$$y'' + \left(\frac{\nu_0}{R}\right)^2 y = \frac{F_y}{m\gamma\beta^2 c^2}, \tag{1.20}$$

where ν_0 is the unperturbed tune and the factor of $1/\gamma$ on the right-hand side represents the rigidity of the particle and F_y is given by Eq. (1.19). In terms of the classical radius of the particle r_0, we have the prescription of Eq. (1.13) with $K = 2\lambda r_0/a^2\beta^2\gamma^3$.

For small tune shifts $\Delta\nu = \nu - \nu_0$, we obtain, from Eq. (1.16), an expression for the *space charge tune shift*,

$$\Delta\nu = -\frac{\lambda r_0 R^2}{\nu_0 a^2 \beta^2 \gamma^3}. \tag{1.21}$$

The negative sign indicates that the direct space charge is defocusing. The same tune shift also occurs in the horizontal dimension provided ν_0 is interpreted as the horizontal unperturbed tune. In a strong focusing accelerator, one has the connection $\epsilon = a^2/2\beta_y$, where ϵ is the transverse emittance of the beam and in the smooth accelerator model is equal to $\nu_0 a^2/2R$. In the case of a proton beam, the emittance usually depends on beam energy in such a way that the normalized emittance $\epsilon_N \equiv \epsilon\beta\gamma$ is a constant even during acceleration when β and γ change. It would then be convenient to express Eq. (1.21) in terms of ϵ_N,

$$\Delta\nu = -\frac{\lambda r_0 R}{2\epsilon_N \beta\gamma^2}. \tag{1.22}$$

The tune shift $\Delta\nu$ specifies the limit of space charge effect on beam intensity. In a beam transport line, for example, defocusing due to space charge force must not be larger than the focusing provided by external focusing elements, i.e., $|\Delta\nu|$ must be less than ν_0. This leads to a stability limit on the beam current $I = e\lambda\beta c$ given by

$$I < \frac{2ec\beta^2\gamma^2\epsilon_N}{r_0\beta_y}. \tag{1.23}$$

In Eq. (1.23), $2\pi\beta_y$ is the average betatron wavelength in the transport line.

The stability condition imposed by space charge tune shift in circular accelerators is slightly different from that for transport lines. In a circular accelerator, the tune shift, Eq. (1.22), must not cause the tune value to cross a low order rational number where resonant effects cause the beam to become unstable. A typical value of this limit is approximately 0.5 to avoid major resonances; in other words, beam stability requires $|\Delta\nu| \lesssim 0.5$.[13] Note that $\Delta\nu$ is inversely proportional to $\beta\gamma^2$. The space charge effect decreases rapidly with increasing beam energy. Note also $\Delta\nu$ is proportional to the circumference of the accelerator, indicating a preference for a compact accelerator design.

[13]J. P. Delahaye et al., *Proc. 11th Int. Conf. on High Energy Accelerators*, Geneva, 1980, p. 299; E. Raka et al., IEEE Trans. Nucl. Sci. **NS-32**, 3110 (1985); C. Ankenbrandt and S. D. Holmes, *Proc. IEEE Conf. Part. Accel.*, Washington, 1987, p. 1066.

In the case of a bunched beam, Eq. (1.22) gives the maximum space charge tune shift if one takes λ to be $\hat{\lambda}$, the peak line charge density near the center of the beam bunch. For Gaussian beams, this means $\hat{\lambda} = N/\sqrt{2\pi}\sigma_z$. Take a proton synchrotron, for example, with $\epsilon_N = 1 \times 10^{-6}$ m, $R = 60$ m, $N = 10^{10}$, $\sigma_z = 0.3$ m, and $\nu_0 \approx 8$; one finds a beam size of $a = 3.8$ mm and a maximum tune shift of $\Delta\nu = -0.4$ at a beam momentum of 1 GeV/c. The electric field at the beam edge ($r = a$) is about 10 kV/m.

Exercise 1.1 Derive an expression of $\Delta\nu$ for a round Gaussian beam of rms transverse size σ. Consider small oscillation amplitudes. Show that the result is given by Eq. (1.22) if we replace a by $\sqrt{2}\sigma$ and define $\epsilon = \sigma^2/\beta_y$.

The cancellation between the electric and magnetic forces, and thus the nonrelativistic nature of the direct space charge effect, is a consequence of considering the beam in free space. When boundary conditions are included, this cancellation is destroyed, leading to a potentially much larger tune shift for relativistic beams.[14]

To illustrate this, consider the previous uniform unbunched beam in a vacuum chamber modeled as two parallel plates (made of perfectly conducting, nonmagnetic metal) located at vertical positions $y = h$ and $y = -h$. The boundary condition is such that the electric field is perpendicular to the plates. The electric field now contains, in addition to Eq. (1.17), a contribution from the image charges. Assuming $h \gg a$, the image charge contribution can be calculated as coming from a series of image line charges of density $-\lambda e$ at $y = \pm 2h, \pm 6h, \pm 10h, \ldots$, and density λe at $y = \pm 4h, \pm 8h, \ldots$, as shown in Figure 1.6(a). A particle at location y on the y-axis will experience an electric field, due to image charges, of

$$E_y = 2\lambda e\left(\frac{1}{2h - y} - \frac{1}{4h - y} + \frac{1}{6h - y} - \cdots - \frac{1}{2h + y} + \frac{1}{4h + y} - \frac{1}{6h + y} + \cdots\right). \tag{1.24}$$

For $|y| \ll h$, this gives, to first order in y,

$$E_y \approx -\frac{\lambda e}{h^2} y \sum_{n=1}^{\infty} \frac{(-1)^n}{n^2} = \frac{\pi^2}{12}\frac{\lambda e}{h^2} y. \tag{1.25}$$

The boundary condition for the static magnetic field is determined by the magnet pole faces (made of ferromagnetic material) instead of the vacuum chamber. Let the boundary be represented as two parallel plates located at

[14] L. J. Laslett, *Proc. Summer Study on Storage Rings, Accelerators, and Experimentation at Super-high Energies*, 1963, BNL Report 7534, p. 324.

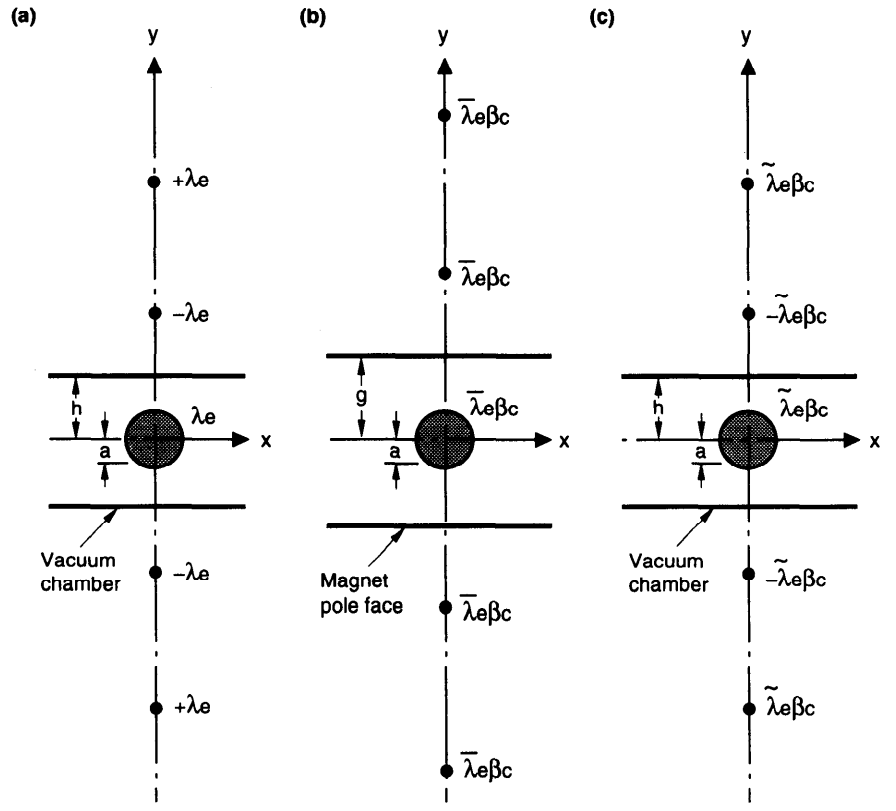

Figure 1.6. (a) Image charges due to a line charge density λe in a two-parallel-plate vacuum chamber. (b) Image currents due to a dc line current $\bar{\lambda} e\beta c$. (c) Image currents due to an ac line current $\tilde{\lambda} e\beta c$. The beam size a is assumed to be much smaller than the vacuum chamber pipe gap h and the magnet pole face spacing g ($g > h$, so that the vacuum chamber fits inside the magnet gap).

$y = g$ and $y = -g$. The boundary condition is that the magnetic field is perpendicular to the magnet pole faces. The image currents are $+\lambda e\beta c$ at $y = \pm 2g, \pm 4g, \pm 6g, \ldots$, yielding a magnetic field, seen by a particle at location y on the y-axis, equal to

$$B_x = 2\lambda e\beta\left(\frac{1}{2g-y} + \frac{1}{4g-y} + \frac{1}{6g-y} + \cdots - \frac{1}{2g+y} - \frac{1}{4g+y} - \frac{1}{6g+y} - \cdots\right)$$

$$\approx \frac{\lambda e\beta}{g^2} y \sum_{n=1}^{\infty} \frac{1}{n^2} = \frac{\pi^2}{6}\frac{\lambda e\beta}{g^2} y. \tag{1.26}$$

The successive image charges have alternating signs, but the image currents all have the same sign. Adding the image force $F_y = e(E_y + \beta B_x)$ to the direct space charge force, one obtains a vertical tune shift

$$\Delta\nu_y = -\frac{\lambda r_0 R^2}{\nu_{y0}\beta^2\gamma}\left(\frac{1}{a^2\gamma^2} + \frac{\pi^2}{24h^2} + \frac{\pi^2\beta^2}{12g^2}\right). \tag{1.27}$$

The first term comes from the direct space charge. The other two terms come from the image charges and currents, respectively. All these contributions are defocusing. The image contributions dominate if $\gamma > h/a$ or g/a. When h and g terms are removed, the expression reduces to the free space result, Eq. (1.21).[15]

Exercise 1.2 Equations (1.24–1.27) are for the y-motion. Repeat the analysis for the x-motion. Show that, for small amplitudes,

$$E_x = -\frac{\pi^2}{12}\frac{\lambda e}{h^2}x \quad \text{and} \quad B_y = \frac{\pi^2}{6}\frac{\lambda e\beta}{g^2}x. \tag{1.28}$$

Note that the fields due to the image charges and currents satisfy $\nabla \cdot \vec{E} = 0$ and $\nabla \times \vec{B} = 0$. Show that the horizontal tune shift is given by

$$\Delta\nu_x = -\frac{\lambda r_0 R^2}{\nu_{x0}\beta^2\gamma}\left(\frac{1}{a^2\gamma^2} - \frac{\pi^2}{24h^2} - \frac{\pi^2\beta^2}{12g^2}\right). \tag{1.29}$$

Equations (1.27) and (1.29) are applicable for an unbunched beam. As mentioned before, for a direct space charge effect, all we need to do for a bunched beam is to replace λ by $\hat{\lambda}$ to obtain the maximum tune shift. In case there is a boundary, the maximum electric field is still obtained by replacing λ by $\hat{\lambda}$, but the calculation of magnetic field is more involved. One has to decompose the current into a "dc" component $\bar{\lambda}$ and an "ac" component $\tilde{\lambda}$, where the dc component contains frequencies at which the skin depth is greater than the vacuum chamber pipe wall thickness, while the ac component has a skin depth that is small compared to the pipe thickness.[16] The boundary condition at $y = \pm g$ as was done to obtain the magnetic field (1.26) is to be applied to $\bar{\lambda}$. The boundary condition for $\tilde{\lambda}$ is that the magnetic field is parallel to the vacuum chamber walls at $y = \pm h$. The corresponding image currents are shown in Figure 1.6(c). Note that the successive images have alternating signs.

[15] For more general beam and vacuum chamber geometries, see B. W. Zotter, IEEE Trans. Nucl. Sci. **NS-22**, 1451 (1975).

[16] See Eq. (2.7) for a definition of the skin depth δ_{skin}. Strictly speaking, if the pipe is perfectly conducting, $\delta_{skin} = 0$, and all currents are ac.

If we identify $\bar{\lambda}$ as the average beam density and $\tilde{\lambda}$ as $\hat{\lambda} - \bar{\lambda}$, following Laslett,[17] and apply the proper boundary conditions, the vertical tune shift is found to be

$$\Delta\nu_y = -\frac{r_0 R^2}{\nu_{y0}\beta^2\gamma}\left[\frac{1}{\gamma^2}\left(\frac{1}{a^2} + \frac{\pi^2}{24h^2}\right)\hat{\lambda} + \beta^2\left(\frac{\pi^2}{24h^2} + \frac{\pi^2}{12g^2}\right)\bar{\lambda}\right] \quad (1.30)$$

The first term, containing $\hat{\lambda}/a^2$, is the direct space charge term, Eq. (1.21). Terms proportional to $\hat{\lambda}$ are suppressed by $1/\gamma^2$, but the $\bar{\lambda}$-terms are not similarly suppressed. For a beam of M Gaussian bunches, each containing N particles, we have $\bar{\lambda} = MN/2\pi R$ and $\hat{\lambda} = N/\sqrt{2\pi}\sigma_z$. For a highly bunched beam, the image effects dominate if γ is larger than $\sqrt{\hat{\lambda}/\bar{\lambda}}$ times g/a or h/a. For an unbunched beam with $\hat{\lambda} = \bar{\lambda}$, we recover Eq. (1.27). For perfectly conducting plates at $y = \pm h$, $\bar{\lambda} = 0$ because all currents are ac; the tune shift then acquires the relativistic suppression factor of $1/\gamma^2$.

The above analysis can be carried out similarly for the x-motion. The result is

$$\Delta\nu_x = -\frac{r_0 R^2}{\nu_{x0}\beta^2\gamma}\left[\frac{1}{\gamma^2}\left(\frac{1}{a^2} - \frac{\pi^2}{24h^2}\right)\hat{\lambda} - \beta^2\left(\frac{\pi^2}{24h^2} + \frac{\pi^2}{12g^2}\right)\bar{\lambda}\right]. \quad (1.31)$$

Continuing the numerical example that followed Eq. (1.23) and taking $M = 120$, $\nu_{x0} \approx \nu_{y0} \approx 8$, $g = 7$ cm, and $h = 5$ cm, we find that the image contributions to the tune shifts are $\Delta\nu_{x,y} = \pm 0.0014$, much smaller than the direct space charge contributions.

Equations (1.30–1.31) are known as the *Laslett tune shifts*. The focusing and defocusing properties of the various contributions are summarized in Table 1.1.

So far we have studied the motion of a single particle in an established beam distribution. This is an incoherent effect obtained by assuming the beam distribution is rigid, unperturbed by the motion of single particles. There are also collective effects that perturb the coherent motion of the beam distribution. Such effects will be discussed as we proceed.

For later use, we include here a calculation of the electromagnetic field generated by a perturbed beam distribution. The starting point of this calculation is Eq. (1.8). Consider a beam whose distribution contains a perturbation in the form of a $\cos m\theta$ ring multipole similar to Eq. (1.7) except that $\delta(s - ct)$ is replaced by a general distribution $\lambda(s - ct)$. Let the perturbed beam go down the axis of a perfectly conducting cylindrical pipe of radius b.

[17]This assumes δ_{skin}, evaluated at the revolution frequency, is much smaller than the wall thickness.

By superposition, the transverse fields are given by Eq. (1.8) in the ultrarelativistic limit with the same replacement $\delta(s - ct) \to \lambda(s - ct)$. If we back off from the ultrarelativistic limit but still keep $\gamma \gg 1$ and let the longitudinal distribution be given by $\lambda(s - \beta ct)$, the effect on the electric field is negligible. The magnetic field components become $B_\theta = \beta E_r$ and $B_r = -\beta E_\theta$. The transverse Lorentz force generated by the beam and seen by a test charge e located at (r, θ, s) that moves with the beam is given by

$$\vec{F}_\perp = e\left(\vec{E} + \beta\hat{s} \times \vec{B}\right)_\perp = \frac{e\vec{E}_\perp}{\gamma^2}$$

$$= \frac{2eI_m}{(1 + \delta_{m0})\gamma^2}\lambda(s - \beta ct)$$

$$\times \begin{cases} \left(\dfrac{1}{b^{2m}} - \dfrac{1}{a^{2m}}\right) r^{m-1}(\hat{r}\cos m\theta - \hat{\theta}\sin m\theta), \\ \dfrac{1}{r^{m+1}}(\hat{r}\cos m\theta + \hat{\theta}\sin m\theta) + \dfrac{r^{m-1}}{b^{2m}}(\hat{r}\cos m\theta - \hat{\theta}\sin m\theta), \end{cases} \tag{1.32}$$

where the two entries are for the $r < a$ and the $a < r < b$ regions respectively, and $\hat{r}$ and $\hat{\theta}$ are the directional unit vectors.

There is no transverse force in the beam region ($r < a$) for the case of $m = 0$, as shown already in Figure 1.3(a). For $m = 1$, the transverse force $\vec{F}_\perp$ is uniform across the transverse beam distribution. Implications of Eq. (1.32) on the collective beam instabilities will be studied in later chapters.

Table 1.1. Focusing and defocusing properties of the various space-charge contributions on the horizontal and vertical betatron oscillations. (F means focusing and D means defocusing)

	Horizontal	Vertical
Direct space charge:		
Electric	D	D
Magnetic	F	F
Net	D	D
Image charges and currents:		
Electric	F	D
Dc magnetic	F	D
Ac magnetic	D	F
Net	F	D

Exercise 1.3 Consider a transverse r-distribution that is not $\delta(r - a)$ but a general distribution $n(r)$:

$$\rho_m = \frac{2I_m}{1 + \delta_{m0}} \lambda(s - \beta ct) n(r) \cos m\theta \tag{1.33}$$

with the normalization $\int_0^\infty 2\pi r^{m+1}\, dr\, n(r) = 1$ and I_m the mth moment. Show that, by superposition,

$$\vec{F}_\perp = \frac{2eI_m}{(1 + \delta_{m0})\gamma^2} \lambda(s - \beta ct) \times \left\{ (\hat{r} \cos m\theta + \hat{\theta} \sin m\theta) \frac{1}{r^{m+1}} \int_0^r 2\pi r'^{m+1}\, dr'\, n(r') + (\hat{r} \cos m\theta - \hat{\theta} \sin m\theta) r^{m-1} \left[\frac{1}{b^{2m}} - \int_r^\infty 2\pi\, dr' \frac{n(r')}{r'^{m-1}} \right] \right\}. \tag{1.34}$$

In particular, for a uniform disk distribution with $n(r) =$ constant for $r < a$, the force inside the beam region ($r < a$) is

$$\vec{F}_\perp = \frac{2eI_m}{(1 + \delta_{m0})\gamma^2} \lambda(s - \beta ct) \times \left\{ (\hat{r} \cos m\theta + \hat{\theta} \sin m\theta) \frac{r}{a^{m+2}} + (\hat{r} \cos m\theta - \hat{\theta} \sin m\theta) \times \left[\frac{r^{m-1}}{b^{2m}} + \frac{m + 2}{m - 2} \left(\frac{r^{m-1}}{a^{2m}} - \frac{r}{a^{m+2}} \right) \right] \right\}. \tag{1.35}$$

For $m = 0$, this reduces to Eq. (1.19).

1.5 LONGITUDINAL SPACE CHARGE EFFECTS

The previous section deals with the transverse effects of the space charge force. For an unbunched beam with uniform longitudinal distribution, the electric and magnetic fields are purely transverse by symmetry. There are no longitudinal fields and no longitudinal forces. In case the longitudinal distribution is not uniform, but given by $e\lambda(s - \beta ct)$, longitudinal fields no longer vanish. Furthermore, we know that in free space or a perfectly conducting smooth pipe, there will be no longitudinal force in the ultrarelativistic limit.

This is an indication that the longitudinal force is proportional to $1/\gamma^2$. In this section, we will calculate this longitudinal force, which we will show is proportional to $\lambda'(s - \beta ct)/\gamma^2$, where a prime means taking the derivative with respect to s. The longitudinal force vanishes for a uniform beam because $\lambda' = 0$.

Consider a beam of radius a inside a cylindrical, perfectly conducting smooth pipe of radius b. Let the beam be ring-shaped similar to Eq. (1.7) with $m = 0$. The transverse electric and magnetic fields are approximately given by

$$E_r = \frac{B_\theta}{\beta} = 2e\lambda(s - \beta ct)\begin{cases} 0 & \text{if } r < a, \\ 1/r & \text{if } a < r < b. \end{cases} \tag{1.36}$$

Equation (1.36) is valid if the longitudinal spread of the field at the wall due to the $1/\gamma$ opening angle in Figure 1.2(a) is small compared with the distance over which the longitudinal distribution changes appreciably.[18] In this case, E_r and B_θ are determined by the *local* longitudinal beam density where the field is evaluated.

We next calculate the longitudinal electric field by applying Faraday's law

$$\oint d\vec{l} \cdot \vec{E} = -\frac{1}{c}\frac{\partial}{\partial t}\int d\vec{\mathscr{A}} \cdot \vec{B} \tag{1.37}$$

to the circuit shown in Figure 1.7(a). One of the sides of the circuit is on the pipe axis and the opposite side is just inside the perfectly conducting pipe wall where the longitudinal electric field component vanishes. The length of these two sides is Δs, which is considered infinitesimal. Application of Eq. (1.37) gives a condition for the longitudinal electric field E_s on the pipe axis:

$$E_s \Delta s + 2e[\lambda(s + \Delta s - \beta ct) - \lambda(s - \beta ct)]\int_a^b \frac{dr}{r}$$
$$= -\frac{2e\beta}{c}\frac{\partial \lambda(s - \beta ct)}{\partial t}\Delta s \int_a^b \frac{dr}{r}. \tag{1.38}$$

By connecting $\partial\lambda/\partial t = -\beta c\lambda'$, Eq. (1.38) gives

$$E_s = -\frac{2e}{\gamma^2}\lambda'(s - \beta ct)\ln\frac{b}{a}. \tag{1.39}$$

One can draw the circuit with the axis side off axis but still inside the beam, as shown in Figure 1.7(b). It follows that Eq. (1.39) applies to the region $r < a$, because E_r and B_θ vanish inside the beam. We thus conclude that E_s is constant, given by Eq. (1.39), inside the beam cross

[18] For a bunched beam with length l, this means $l \gg b/\gamma$. See Exercises 1.4 and 1.5 below.

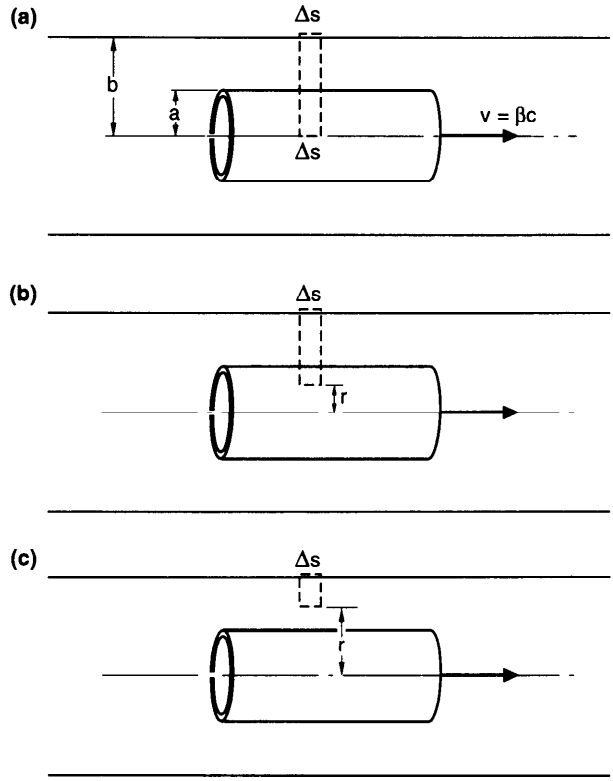

Figure 1.7. The longitudinal electric field can be calculated by drawing the various circuits as shown and applying Faraday's law. The cylinders represent the ring beam. These calculations are applied to both $m = 0$ and $m \neq 0$. The circuits are drawn in the $\theta = 0$ plane.

section. One can also place the axis side of the circuit outside the beam as shown in Figure 1.7(c), which yields, in the region $a < r < b$,

$$E_s = -\frac{2e}{\gamma^2}\lambda'(s - \beta ct)\ln\frac{b}{r}. \tag{1.40}$$

When $r = b$, this gives $E_s = 0$. Equations (1.36), (1.39), and (1.40) complete the field components; the rest of the field components E_θ, B_r, and B_s vanish.

As promised, the longitudinal force $F_s = eE_s$ is proportional to λ'/γ^2. Physically the force comes from an imbalance between the amounts of charge behind and in front of the test charge being considered. In case there are more charges in the front, λ' is positive, leading to a retarding force. In case there are more charges in back, the force is accelerating.

Exercise 1.4 Show that the approximate expressions (1.36), (1.39) and (1.40) satisfy the Maxwell equations if $\lambda \gg \lambda'' b^2/\gamma^2$. For a bunched beam, this requires the bunch length l to be much longer than b/γ. Show that the leading correction term to Eq. (1.36) is

$$\Delta E_r = \frac{\Delta B_\theta}{\beta} = \frac{e}{\gamma^2}\lambda''(s-\beta ct)\begin{cases} r\ln\dfrac{b}{a}, \\ r\ln\dfrac{b}{r} + \dfrac{r}{2} - \dfrac{a^2}{2r}, \end{cases} \tag{1.41}$$

where the two entries refer to the regions $r < a$ and the $a < r < b$, respectively.

Exercise 1.5 The above analysis was done in the presence of a beam pipe. Removing the beam pipe by setting $b \to \infty$ gives an apparent logarithmic divergence of E_s in free space. However, the analysis breaks down when b becomes comparable to γl. To illustrate this explicitly, consider the case of free space without a beam pipe. The longitudinal electric field at position z on the axis can be obtained by superposing contributions from infinitesimal rings. Show that

$$E_s(z) = -\frac{1}{\gamma^2}\int_{-\infty}^{\infty} e\lambda(z'-z)\,dz' \frac{z'}{\left(z'^2 + \dfrac{a^2}{\gamma^2}\right)^{3/2}}. \tag{1.42}$$

Consider the case with $\lambda(z) = (1/2l)(1 + z/l)$ for $|z| < l$, and 0 for $|z| > l$, which gives $\lambda' = 1/2l^2$. Assuming $\gamma l \gg a$, show that at the bunch center $E_s(0)$ is given by Eq. (1.39) with b replaced by γl.

In case the transverse distribution is not ring-shaped, but described by $n(r)$ [normalized by $\int_0^\infty 2\pi r\,dr\,n(r) = 1$], superposition gives

$$E_s = -\frac{2e}{\gamma^2}\lambda'(s-\beta ct)\left[\ln\frac{b}{r} - \int_r^b 2\pi r'\,dr'\,n(r')\ln\frac{r'}{r}\right]. \tag{1.43}$$

This E_s vanishes if $r = b$, as it should. In case the transverse beam distribution $n(r)$ is uniform in region $r < a$, the field is

$$E_s = -\frac{2e}{\gamma^2}\lambda'(s-\beta ct)\begin{cases} \ln\dfrac{b}{a} + \dfrac{1}{2} - \dfrac{r^2}{2a^2}, \\ \ln\dfrac{b}{r}. \end{cases} \tag{1.44}$$

This E_s gives a field on the pipe axis that differs from the ring beam case, Eq. (1.39), as the form factor $\ln(b/a)$ is replaced by $\ln(b/a) + \frac{1}{2}$.

Consider the longitudinal motion of a particle in a bunched beam that has a uniform transverse distribution. Let z be the longitudinal coordinate of the particle relative to the beam center. The longitudinal electric field, Eq. (1.44), will contribute to an energy gain gradient of $eE_s(z)$. From Eq. (1.9), the perturbed equations of motion for the particle is

$$\begin{aligned} z' &= -\eta\delta, \\ \delta' &= \frac{1}{\eta}\left(\frac{\nu_{s0}}{R}\right)^2 z + \frac{eE_s(z)}{\beta^2 E}, \end{aligned} \tag{1.45}$$

where E is the design energy of the accelerator. The factor $1/\beta^2$ comes from the conversion $\Delta P/P = \Delta E/\beta^2 E$. If the longitudinal distribution λ is parabolic in z with total length $2\hat{z}$, the perturbed synchrotron motion is described by

$$z'' + \left(\frac{\nu_{s0}}{R}\right)^2 z = -\frac{3Nr_0\eta}{\beta^2\gamma^3\hat{z}^3}\left(\ln\frac{b}{a} + \frac{1}{2}\right)z. \tag{1.46}$$

The perturbed motion (1.46) is of the type of Eq. (1.13). The synchrotron tune of single-particle motion in the presence of space charge perturbation is therefore given by

$$\nu_s^2 = \nu_{s0}^2 + \frac{3Nr_0\eta R^2}{\beta^2\gamma^3\hat{z}^3}\left(\ln\frac{b}{a} + \frac{1}{2}\right). \tag{1.47}$$

For a small tune shift, we obtain

$$\Delta\nu_s = \frac{3Nr_0\eta R^2}{2\beta^2\gamma^3\hat{z}^3\nu_{s0}}\left(\ln\frac{b}{a} + \frac{1}{2}\right). \tag{1.48}$$

This synchrotron tune shift has the same sign as η. The space charge force is focusing and defocusing according as the operation is above or below transition. This is to be compared with its transverse counterpart, Eq. (1.21), which always defocuses.

Continuing the numerical example that followed Eq. (1.23) and Eq. (1.31), and taking in addition $\eta = (1/\nu_{x0}^2) - (1/\gamma^2) = -0.45$, $\hat{z} = (9\pi/2)^{1/6}\sigma_z = 0.47$ m,[19] $\nu_{s0} = 0.04$, and $b = 5$ cm, the synchrotron tune is found from Eq. (1.47) to be significantly suppressed by the space charge force, from 0.04 to 0.016 in the present example.

[19]The factor $(9\pi/2)^{1/6}$ is chosen to give the same result for small oscillations when λ is Gaussian. See Exercise 3.4 also.

One can extend the analysis to higher multipole distributions with $m \neq 0$. To do so for the case of a ring-shaped beam, we first write down the transverse field components according to Eq. (1.8),

$$E_r = \frac{B_\theta}{\beta} = 2I_m\lambda(s - \beta ct)\cos m\theta \begin{cases} -\left(\frac{1}{a^{2m}} - \frac{1}{b^{2m}}\right) r^{m-1}, \\ \frac{1}{r^{m+1}} + \frac{r^{m-1}}{b^{2m}} \end{cases} \tag{1.49}$$

and

$$E_\theta = -\frac{B_r}{\beta} = 2I_m\lambda(s - \beta ct)\sin m\theta \begin{cases} \left(\frac{1}{a^{2m}} - \frac{1}{b^{2m}}\right) r^{m-1}, \\ \frac{1}{r^{m+1}} - \frac{r^{m-1}}{b^{2m}}. \end{cases} \tag{1.50}$$

If we draw circuits as shown in Figure 1.7(b) and (c) and apply Faraday's law, we obtain the longitudinal electric field

$$E_s = -\frac{2I_m}{m\gamma^2}\lambda'(s - \beta ct)\cos m\theta \begin{cases} \left(\frac{1}{a^{2m}} - \frac{1}{b^{2m}}\right) r^m, \\ \frac{1}{r^m} - \frac{r^m}{b^{2m}}. \end{cases} \tag{1.51}$$

Exercise 1.6

(a) The circuits in Figure 1.7 can also be used to calculate the longitudinal magnetic field by applying Ampere's law $\oint d\vec{l} \cdot \vec{B} = (1/c)(\partial/\partial t)\int d\vec{s} \cdot \vec{E}$, where we have used the fact that there is no contribution from the current source because $j_\theta = 0$. Following similar steps as before, show that B_s vanishes.

(b) Show explicitly that Eqs. (1.49–1.51) satisfy the Maxwell equations, ignoring terms involving λ''.

(c) It is amusing to show that fields for $m \neq 0$ reduce to those for $m = 0$ on setting $I_0 = e$ and taking the limit $m \to 0$, even though strictly m assumes only integral values. [Remember to include the factor $1/(1 + \delta_{m0})$.]

If the beam distribution is that of Eq. (1.33) with a general transverse distribution $n(r)$, the longitudinal electric field is obtained by superposition:

$$E_s = -\frac{2I_m}{m\gamma^2}\lambda'(s - \beta ct)\cos m\theta \times \left[\frac{1}{r^m}\int_0^r 2\pi r'^{m+1}\, dr'\, n(r') + r^m\int_r^b \frac{2\pi\, dr'\, n(r')}{r'^{m-1}} - \frac{r^m}{b^{2m}}\right]. \tag{1.52}$$

For uniform $n(r)$ up to radius $r = a$, the result is

$$E_s = -\frac{2I_m}{m\gamma^2}\lambda'(s-\beta ct)\cos m\theta \times \begin{cases} -r^m\left(\dfrac{1}{b^{2m}} + \dfrac{m+2}{m-2}\dfrac{1}{a^{2m}}\right) + \dfrac{2m}{m-2}\dfrac{r^2}{a^{m+2}}, \\ \dfrac{1}{r^m} - \dfrac{r^m}{b^{2m}}. \end{cases} \tag{1.53}$$

Comparing Eqs. (1.32) and (1.51), we find the ratio of longitudinal to transverse space charge forces is of the order of

$$F_{\parallel}/F_{\perp} \approx \frac{r}{m}\frac{\lambda'}{\gamma^2}\Big/\frac{\lambda}{\gamma^2}. \tag{1.54}$$

Both transverse and longitudinal space charge forces, being proportional to $1/\gamma^2$, are nonrelativistic effects. In the transverse case, it comes from the less than perfect cancellation between the electric and the magnetic forces. In the longitudinal case, it is due to Lorentz contraction. In case the bunch length is much longer than its transverse size, the longitudinal force is much weaker than the transverse force.

We have assumed in our treatment that all beam particles have the same energy. As an illustration of one mechanism which causes a spread of particle energies, consider the device sketched in Figure 1.8. Suppose all particles have the same energy when produced at the gun. Let the transverse focusing be provided by a longitudinal magnetic field $B_s = \infty$ so that all particles move strictly in the $\hat{s}$-direction. Sufficiently away from the gun, the beam reaches an equilibrium state. Let the transverse distribution in this equilibrium state be that of a uniform disk of radius a, and let the longitudinal density be λ. A transverse electric field E_r given by Eq. (1.17) is established, and the energy of a particle, $m_0c^2\gamma$, becomes dependent on its radial position r relative to

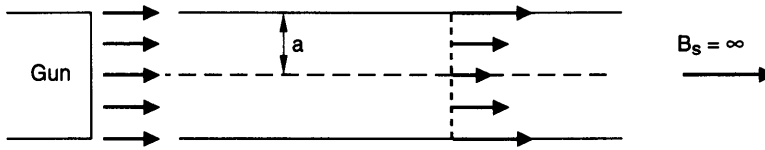

Figure 1.8. Illustration of an energy depression mechanism. All particles are produced with equal energies at the gun, which is maintained at a constant potential, but sufficiently downstream from the gun, particles at the beam center acquire an energy depression $\Delta\gamma = -\lambda r_0$ relative to particles at the beam edge.

the beam center. We have by energy conservation

$$m_0c^2\gamma(r) = m_0c^2\gamma(0) + e\int_0^r dr' E_r(r'). \tag{1.55}$$

A particle at the beam center has a lower energy than a particle at the beam edge. The energy of a particle at radius r is given by

$$\gamma(r) = \gamma(0) + \lambda r_0 \frac{r^2}{a^2}. \tag{1.56}$$

Equation (1.56) thus describes one mechanism for the beam to acquire an energy spread sufficiently downstream from the gun even when all particles are produced monoenergetic at the gun. Our treatment of space charge effects ignores the beam energy spread, and it applies if

$$\lambda r_0 \ll \gamma. \tag{1.57}$$

When $\lambda r_0 \gtrsim \gamma$, the center particles will come to a halt at some distance from the gun. This constitutes a limit on the beam intensity.[20]

1.6 ENVELOPE EQUATION

The previous two sections were developed in the context of circular accelerators. The space charge forces also have an effect on linacs or beam transport lines. The longitudinal space charge force causes an energy difference between the head and the tail of a beam bunch. The transverse space charge force perturbs the externally applied focusing force that confines the beam. The longitudinal effect on beam energy spread will be discussed later in Eq. (3.9). The transverse effect will be investigated in this section in terms of the envelope equation.[21]

Consider a transport line for a proton or heavy-ion beam which has a high intensity and a medium energy. The proton line may be one that is used to transport the proton beam from a linac to a synchrotron for further acceleration to higher energies. The heavy-ion line may be used as a driver for inertial confinement fusion. Let the beam particle have a charge Qe and a mass which is A times the proton mass. We suppose the beam is continuous, with a uniform longitudinal particle density λ. In case of a bunched beam, we

[20]See for example J. D. Lawson, *The Physics of Charged-Particle Beams*, Clarendon Press, Oxford, 1977.

[21]I. M. Kapchinskij and V. V. Vladimirskij, *Proc. 2nd Int. Conf. on High Energy Accel. and Instr.*, CERN, 1959, p. 274.

consider λ to be the maximum local density. We also suppose the externally applied forces are linear in the transverse displacements x and y, and we ignore the effects of vacuum chamber walls.

Consider a beam distribution in the four-dimensional transverse phase space (x, p_x, y, p_y) that lies on a δ-function shell as

$$\psi(x, p_x, y, p_y) = \frac{Qe\lambda}{\pi^2 \epsilon_x \epsilon_y} \delta\left(\frac{x^2}{a^2} + \frac{a^2 p_x^2}{\epsilon_x^2} + \frac{y^2}{b^2} + \frac{b^2 p_y^2}{\epsilon_y^2} - 1 \right), \quad (1.58)$$

which is normalized by

$$\int dx\, dp_x\, dy\, dp_y\, \psi = Qe\lambda. \quad (1.59)$$

The distribution (1.58) was introduced by Kapchinskij and Vladimirskij and is called the *KV distribution*. It has the property that when projected onto any two of the four phase space dimensions, one obtains a uniform elliptical distribution. For example, the projection onto the x-y plane is

$$\psi(x, y) = \frac{Qe\lambda}{\pi ab} H\left(1 - \frac{x^2}{a^2} - \frac{y^2}{b^2} \right), \quad (1.60)$$

where $H(u) = 1$ if $u > 0$ and 0 if $u < 0$ is the step function. Equation (1.60) gives a uniform elliptical distribution with horizontal and vertical extents a and b. The parameters $\epsilon_{x,y}$ in Eq. (1.58) are the horizontal and vertical beam emittances at the edge of the envelopes.

The electric field at position (x, y) produced by the beam charge is obtained by integrating over the beam distribution,

$$\vec{E}(x, y) = \frac{2Qe\lambda}{\pi ab} \iint_{1 > (x'/a)^2 + (y'/b)^2} dx'\, dy' \, \frac{(x - x')\hat{x} + (y - y')\hat{y}}{(x - x')^2 + (y - y')^2}. \quad (1.61)$$

The double integral in Eq. (1.61) can be evaluated—the algebra is lengthy but straightforward—to yield, for positions inside the beam distribution,

$$\vec{E}(x, y) = 4Qe\lambda \left[\frac{x}{a(a + b)} \hat{x} + \frac{y}{b(a + b)} \hat{y} \right]. \quad (1.62)$$

The space charge force must also include the magnetic force, which almost cancels the electric force for relativistic beams. When included, the net Lorentz force on a particle at position (x, y) is equal to the electric force

divided by γ^2, i.e.,

$$\vec{F}(x, y) = \frac{4Q^2e^2\lambda}{\gamma^2}\left[\frac{x}{a(a+b)}\hat{x} + \frac{y}{b(a+b)}\hat{y}\right]. \tag{1.63}$$

The KV model is notable because it offers a self-consistent picture. It gives a uniform elliptical beam distribution in the x-y plane; this distribution gives a linear space charge force in x and y inside the distribution; the linear forces in turn make it possible for the beam to maintain the four-dimensional ellipsoidal distribution it started out with. Therefore, the complex self-consistency problem is reduced to solving the dynamics of the two beam envelope parameters a and b.

In the presence of the space charge force (1.63), the single-particle equations of motion are

$$\begin{aligned} x'' + \left[K_x(s) - \frac{\xi}{a(a+b)}\right]x = 0, \\ y'' + \left[K_y(s) - \frac{\xi}{b(a+b)}\right]y = 0, \end{aligned} \tag{1.64}$$

where a prime means taking the derivative with respect to s, $K_{x,y}(s)$ specifies the external focusing, and

$$\xi = \frac{4Q^2r_0\lambda}{A\beta^2\gamma^2} \tag{1.65}$$

is a dimensionless space charge parameter.

We need to find a and b as functions of s by imposing conditions of self-consistency. To do so, consider a particle with the maximum allowed x-amplitude $a(s)$ at location s. This particle does not execute any y-motion, because $x = a$ necessarily means $y = 0$ and $p_y = 0$ in a KV distribution. We first write for this particle

$$x = a(s)\cos\phi_x(s) \tag{1.66}$$

where $\phi_x(s)$ is a certain phase yet to be found. Substituting into the left hand side of Eq. (1.64) results in two terms, one proportional to $\sin\phi_x(s)$ and the other proportional to $\cos\phi_x(s)$. In order for Eq. (1.64) to be valid for all s, both terms must vanish, yielding

$$\begin{aligned} a'' - a(\phi_x')^2 = -\left[K_x(s) - \frac{\xi}{a(a+b)}\right]a, \\ a\phi_x'' + 2a'\phi_x' = 0. \end{aligned} \tag{1.67}$$

The second equation of the pair (1.67) gives

$$\phi_x' \propto \frac{1}{a(s)^2}. \tag{1.68}$$

The proportionality constant is just the emittance ϵ_x, so far unspecified, i.e.,

$$\phi_x' = \frac{\epsilon_x}{a(s)^2}. \tag{1.69}$$

Substituting Eq. (1.69) into the first equation of (1.67) gives the self-consistency condition we are looking for. Similarly, if we start with a particle with the maximum allowed y-amplitude with $y = b\cos\phi_y$, we obtain the other self-consistency condition for $b(s)$. These two conditions constitute the *envelope equations*, as[22]

$$\begin{aligned} a'' + K_x a - \frac{\epsilon_x^2}{a^3} &= \frac{\xi}{a+b}, \\ b'' + K_y b - \frac{\epsilon_y^2}{b^3} &= \frac{\xi}{a+b}. \end{aligned} \tag{1.72}$$

Given the focusing strengths $K_{x,y}(s)$ and the space charge parameter ξ, the nonlinear coupled differential equations (1.72) determine the behavior of the beam envelopes $a(s)$ and $b(s)$.

Exercise 1.7 Show that in the absence of external focusing and space charge forces, the beam envelopes are hyperbolas,

$$a(s) = \sqrt{a_0^2 + \frac{\epsilon_x^2}{a_0^2}(s - s_0)^2}, \tag{1.73}$$

[22]For readers familiar with the β-function language of circular accelerators, Eqs. (1.69) and (1.72) are the transport equivalents of the Courant-Snyder relations

$$\begin{aligned} \phi_x' &= \frac{1}{\beta_x(s)}, \\ 2\beta_x\beta_x'' - (\beta_x')^2 + 4K_x\beta_x^2 &= 4, \end{aligned} \tag{1.70}$$

and their vertical counterparts. The equivalence can be established by the connections

$$a = \sqrt{\epsilon_x \beta_x} \quad \text{and} \quad b = \sqrt{\epsilon_y \beta_y}. \tag{1.71}$$

In this context, the space charge terms are modifications of the focusing strengths $K_{x,y}$, and the envelope equation is just a different form of the second number of Eq. (1.70).

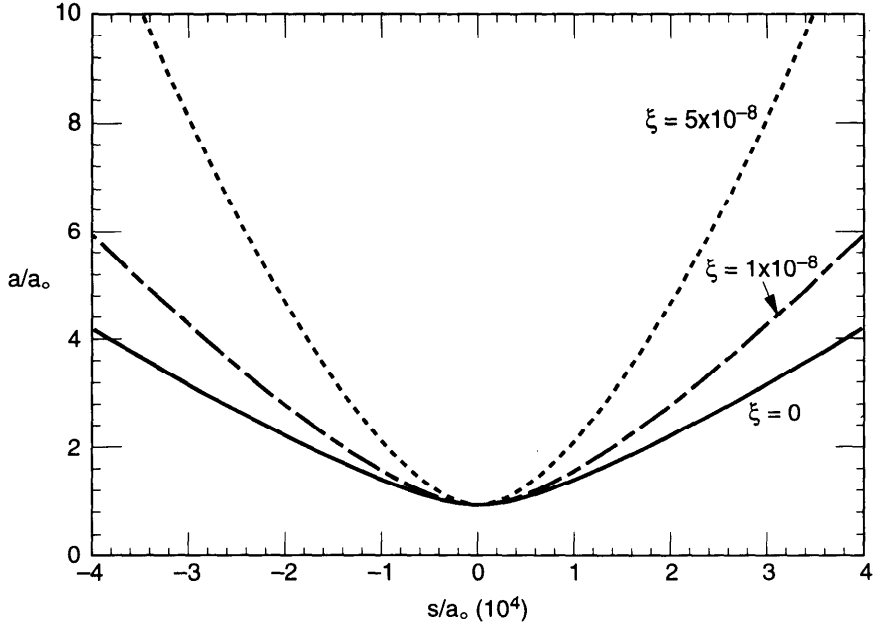

Figure 1.9. The effect of space charge on beam envelope near a beam waist in the absence of external focusing. The graph shows a / a_0 as a function of s / a_0, where a waist $a = a_0$ at $s = 0$ is assumed. The three curves are for $\xi = 0$, 1×10^{-8}, and 5×10^{-8}, and ϵ / a_0 is taken to be 10^{-4}. The case $\xi = 0$ is a hyperbola, Eq. (1.73).

where a_0 is the size of a beam "waist," and s_0 is the location of the waist. Note that a small waist size necessarily implies faster divergence away from the waist.

Exercise 1.8 Set up the envelope equation for a round beam with KV distribution under the influence of the space charge in free space. Solve the equation numerically to obtain $a(s)$ near a waist location. The result is shown in Figure 1.9.

Exercise 1.9 Show that for a round beam, if the focusing is provided by a solenoid magnet of strength B_s, the envelope equation reads

$$a'' + \left(\frac{eB_s}{2E}\right)^2 a - \frac{\epsilon^2}{a^3} = \frac{\xi}{2a}, \tag{1.74}$$

where E is the particle energy, and ϵ is the beam emittance.

Exercise 1.10 The envelope equation (1.72) is derived assuming no acceleration, and thus does not apply to linacs, but it can be modified to include acceleration.

(a) Show that if acceleration is adiabatic, i.e., if $\gamma'/\gamma \ll \beta^2 a'/a$, Eq. (1.69) still holds, and the modified envelope equation reads

$$a'' + \frac{\gamma'}{\beta^2\gamma}a' + K_x a - \frac{\epsilon_x^2}{a^3} = \frac{\xi}{a+b} \tag{1.75}$$

and similarly for b. Note that an extra term, proportional to a' and γ', is introduced, and that ξ, still defined by Eq. (1.65), depends on s through γ and β.

(b) Consider the case of a uniform acceleration, $(\beta\gamma)' = \alpha = \text{const}$. Make the transformation $a = A/\sqrt{\beta\gamma}$ and $b = B/\sqrt{\beta\gamma}$ to show that the envelope equation (1.72) is recovered if we make the replacements

$$\begin{gathered} A \to a, \qquad B \to b, \\ K_{x,y} + \frac{\alpha^2}{4\beta^2\gamma^2} \to K_{x,y}, \\ \beta\gamma\epsilon_{x,y} \to \epsilon_{x,y}, \quad \text{and} \quad \beta\gamma\xi \to \xi. \end{gathered} \tag{1.76}$$

The modification of $K_{x,y}$ is small, and can most likely be dropped for practical cases. The modification of $\epsilon_{x,y}$ is related to the definition of the normalized emittance introduced in Eq. (1.22).

To be more specific, consider a round beam with $a = b$ and $\epsilon_x = \epsilon_y = \epsilon$. Let the external focusing be smooth, $K_x = K_y = (\nu/R)^2$, where $2\pi R/\nu$ is the betatron oscillation wavelength along the transport line.[23] The envelope equation (1.72) gives an equation for the equilibrium beam size a_0,

$$\left(\frac{\nu}{R}\right)^2 a_0 - \frac{\epsilon^2}{a_0^3} - \frac{\xi}{2a_0} = 0. \tag{1.77}$$

In the absence of space charge force, the equilibrium beam size is given by

$$a_0^2 = \frac{\epsilon R}{\nu}, \tag{1.78}$$

which is just Eqs. (1.11) and (1.71) combined. Taking into account the space

[23]Symbols are chosen so results can be applied to a circular accelerator where ν is the betatron tune and $2\pi R$ is the accelerator circumference.

charge force, the equilibrium beam size is given by solving Eq. (1.77):

$$a_0^2 = \frac{\epsilon R}{\nu}\left[\sqrt{1 + \left(\frac{\xi R}{4\nu\epsilon}\right)^2} + \frac{\xi R}{4\nu\epsilon}\right]. \tag{1.79}$$

The beam size is significantly perturbed by the space charge force if

$$\frac{\xi R}{4\nu\epsilon} \gtrsim 1. \tag{1.80}$$

If the beam size becomes larger than the vacuum chamber aperture, there will be a beam loss. Even when the beam stays in the vacuum chamber, the beam distribution in phase space may be too distorted to meet the downstream requirements, whether those are for inertial confinement or for further acceleration in a synchrotron. The case of $\xi = 5 \times 10^{-8}$ in Figure 1.9 has $\xi R/4\nu\epsilon = 1.25$.

For weak beam intensities, when $\xi \ll \nu\epsilon/R$, the perturbation on the equilibrium beam size is

$$\Delta a_0^2 = \frac{\xi R^2}{4\nu^2}. \tag{1.81}$$

If this perturbation is interpreted as a perturbation on the single-particle tune ν according to $a_0^2 = \epsilon R/(\nu + \Delta\nu)$, we obtain an expression for the shift of the single-particle betatron wave number:

$$\frac{\Delta\nu}{R} = -\frac{\xi}{4\epsilon} = -\frac{Q^2\lambda r_0 R}{A\nu a_0^2\beta^2\gamma^3}. \tag{1.82}$$

Equations (1.81–1.82) have the interpretations of the β-function distortion and the betatron frequency shift caused by the space charge force. Equation (1.82) is consistent with Eq. (1.21) obtained earlier.

For an intense, low-energy beam, space charge defocusing may overcome external focusing, rendering the beam unstable. This occurs when

$$\left|\frac{\Delta\nu}{R}\right| \gtrsim \frac{\nu}{R}, \tag{1.83}$$

which is just Eq. (1.80) when Eq. (1.82) is substituted for $\Delta\nu/R$.

The instability (1.83) is most likely at low energies. Take a transport line for 50 MeV protons, for example, with $Q = 1$, $A = 1$, and a peak beam current $\hat{I} = \hat{\lambda}e\beta c = 2$ A, we find $\xi = 7 \times 10^{-6}$. If we further take an unperturbed beam size of $a_0 = 2$ cm, the space charge force is strong enough to overcome an external betatron focusing of focal length $R/\nu = 10$ m.

The beam may execute some collective motion on top of the equilibrium established by Eq. (1.79) or Eq. (1.81). Consider again a weak, round beam. Let the horizontal and vertical beam sizes be

$$a(s) = a_0 + \Delta a(s) \quad \text{and} \quad b(s) = a_0 + \Delta b(s), \tag{1.84}$$

where the perturbations Δa and Δb are considered infinitesimal. With a_0 obeying Eq. (1.77), we need to know how Δa and Δb depends on s.

Substitute Eq. (1.84) into the envelope equation (1.72) and linearize with respect to Δa and Δb. We obtain

$$\begin{aligned} \Delta a'' + \left(\frac{\nu}{R}\right)^2 \Delta a + \frac{3\epsilon^2}{a_0^4}\Delta a + \frac{\xi}{4a_0^2}(\Delta a + \Delta b) = 0, \\ \Delta b'' + \left(\frac{\nu}{R}\right)^2 \Delta b + \frac{3\epsilon^2}{a_0^4}\Delta b + \frac{\xi}{4a_0^2}(\Delta a + \Delta b) = 0. \end{aligned} \tag{1.85}$$

The two beam sizes execute coupled oscillations. These oscillations can be described by a superposition of two modes. Adding the two equations in (1.85) gives

$$(\Delta a + \Delta b)'' + \left[\left(\frac{\nu}{R}\right)^2 + \frac{3\epsilon^2}{a_0^4} + \frac{\xi}{2a_0^2}\right](\Delta a + \Delta b) = 0. \tag{1.86}$$

This equation states that one of the collective modes occurs when Δa and Δb oscillate in phase. Such a mode is designated as a + mode, or a 0-mode. Its oscillation frequency is given by

$$\left(\frac{\nu_+}{R}\right)^2 = \left(\frac{\nu}{R}\right)^2 + \frac{3\epsilon^2}{a_0^4} + \frac{\xi}{2a_0^2}. \tag{1.87}$$

The other mode is obtained by subtracting the two equations in (1.85):

$$(\Delta a - \Delta b)'' + \left[\left(\frac{\nu}{R}\right)^2 + \frac{3\epsilon^2}{a_0^4}\right](\Delta a - \Delta b) = 0. \tag{1.88}$$

This mode describes the beam motion in which Δa and Δb oscillate out of phase, and is designated as the − mode or the π-mode. Its mode frequency is given by

$$\left(\frac{\nu_-}{R}\right)^2 = \left(\frac{\nu}{R}\right)^2 + \frac{3\epsilon^2}{a_0^4}. \tag{1.89}$$

One observes the $-$ mode frequency is not directly affected by the space charge force, because it is independent of ξ. As the horizontal and the vertical beam sizes oscillate out of phase with equal amplitudes, the induced space charge force does not perturb the beam envelopes to first order of the oscillation amplitude. The $-$ mode oscillation of the beam sizes therefore does not respond to the space charge force. The opposite is true in the $+$ mode, where the in-phase oscillation of the beam sizes maximizes the effect of the space charge force.

However, the static, equilibrium space charge force is always present. The mode frequencies (1.87) and (1.89) contain the equilibrium beam size a_0, which depends on ξ according to Eq. (1.79) or (1.81). Both mode frequencies therefore shift with beam intensity. Substituting Eq. (1.81) into (1.87) and (1.89) gives, to first order in ξ,

$$\begin{aligned} \frac{\nu_+}{R} &= 2\frac{\nu}{R} - \frac{\xi}{4\epsilon}, \\ \frac{\nu_-}{R} &= 2\frac{\nu}{R} - \frac{3\xi}{8\epsilon}. \end{aligned} \tag{1.90}$$

Both mode frequencies then shift down with increasing beam intensity. In the unperturbed case, $\xi = 0$, the horizontal and vertical beam size oscillations are uncoupled, and the oscillation frequency is twice the natural betatron frequency.

Exercise 1.11 Consider a flat beam with $a \to \infty$, $\lambda \to \infty$, but $\lambda/a \to$ constant. Find the unperturbed vertical beam size b_0^2, and the first order perturbations of Δb_0^2 and $\Delta\nu_y/R$. Find the collective mode frequency by considering an infinitesimal perturbation on the beam size.

So far we have assumed a KV model (1.58). For more realistic distributions, one has to sacrifice the strict self-consistency and be content with approximate descriptions. This can be done by concentrating on the second moments of the beam[24] and ignoring the effects of higher moments.[25]

Consider a one-dimensional problem which has the single-particle equations of motion

$$x' = p \quad \text{and} \quad p' = -K_x x + f_x, \tag{1.91}$$

[24] F. Sacherer, IEEE Trans. Nucl. Sci. **NS-18**, 1105 (1971).

[25] For discussions of higher moments, see R. L. Gluckstern, R. Chasman, and K. Crandall, *Proc. Nat. Accel. Lab. Linear Accel. Conf.*, Vol. 2, Fermilab, 1970, p. 823; I. Hofmann, L. J. Laslett, L. Smith, and I. Haber, Part. Accel. **13**, 145 (1983). For an application of the envelope equation to circular accelerators, see P. Zhou, J. B. Rosenzweig, and S. Stahl, *Proc. IEEE Part. Accel. Conf.*, San Francisco, 1991, p. 1779.

where f_x is related to the force component F_x by $f_x = F_x/Amc^2\beta^2\gamma$. Let the second moments of the beam be designated as $\langle x^2\rangle$, $\langle xp\rangle$, and $\langle p^2\rangle$, where $\langle\ \rangle$ means taking an average over the beam distribution. The equations of motion of the second moments are

$$\begin{aligned}
\langle x^2\rangle' &= 2\langle xx'\rangle = 2\langle xp\rangle, \\
\langle xp\rangle' &= \langle x'p + xp'\rangle = \langle p^2\rangle - K_x\langle x^2\rangle + \langle xf_x\rangle, \\
\langle p^2\rangle' &= 2\langle pp'\rangle = -2K_x\langle xp\rangle + 2\langle pf_x\rangle.
\end{aligned} \tag{1.92}$$

The first two expressions in Eq. (1.92) can be combined to give

$$\langle x^2\rangle'' = 2\langle p^2\rangle - 2K_x\langle x^2\rangle + 2\langle xf_x\rangle. \tag{1.93}$$

Defining the rms beam emittance by [also see Eq. (4.76)]

$$\epsilon_{x,\text{rms}}^2 = \langle x^2\rangle\langle p^2\rangle - \langle xp\rangle^2, \tag{1.94}$$

we can express $\langle p^2\rangle$ in terms of the emittance as

$$\langle p^2\rangle = \frac{\epsilon_{x,\text{rms}}^2}{\langle x^2\rangle} + \frac{\langle xp\rangle^2}{\langle x^2\rangle} = \frac{\epsilon_{x,\text{rms}}^2}{\langle x^2\rangle} + \frac{\left(\langle x^2\rangle'\right)^2}{4\langle x^2\rangle}, \tag{1.95}$$

where use has been made of the first entry of Eq. (1.92). Substituting Eq. (1.95) into Eq. (1.93) and rewriting the result in terms of the rms beam size $\sigma_x = \sqrt{\langle x^2\rangle}$, we obtain

$$\sigma_x'' + K_x\sigma_x - \frac{\epsilon_{x,\text{rms}}^2}{\sigma_x^3} = \frac{\langle xf_x\rangle}{\sigma_x}. \tag{1.96}$$

Similarly, we have

$$\sigma_y'' + K_y\sigma_y - \frac{\epsilon_{y,\text{rms}}^2}{\sigma_y^3} = \frac{\langle yf_y\rangle}{\sigma_y}. \tag{1.97}$$

In the case of the KV model, the force components F_x and F_y are given by Eq. (1.63), and one obtains

$$\begin{aligned}
\sigma_x'' + K_x\sigma_x - \frac{\epsilon_{x,\text{rms}}^2}{\sigma_x^3} &= \frac{\xi}{4(\sigma_x + \sigma_y)}, \\
\sigma_y'' + K_y\sigma_y - \frac{\epsilon_{y,\text{rms}}^2}{\sigma_y^3} &= \frac{\xi}{4(\sigma_x + \sigma_y)},
\end{aligned} \tag{1.98}$$

which is the same as Eq. (1.72), since for the KV model, one has $\epsilon_{x,y} = 4(\epsilon_{x,y})_{\text{rms}}$, $a = 2\sigma_x$, and $b = 2\sigma_y$.

Equations (1.96–1.97) are valid for general beam distributions. In general, the forces F_x and F_y are nonlinear in x and y, and the quantities $\langle xf_x \rangle$ and $\langle yf_y \rangle$ involve moments higher than the second moments. The problem is therefore not closed. However, to the extent that the higher moments can be ignored, we keep only the linear terms (linear in x and y) in $f_{x,y}$; $\langle xf_x \rangle$ and $\langle yf_y \rangle$ can be expressed in terms of the second moments only, and we recover a closed system of equations as in the KV model.

Exercise 1.12 Apply Eqs. (1.96–1.97) to a Gaussian beam

$$\psi(x, p_x, y, p_y) = \frac{Qe\lambda\beta_x\beta_y}{4\pi^2\sigma_x^2\sigma_y^2} \exp\left(-\frac{x^2 + \beta_x^2 p_x^2}{2\sigma_x^2} - \frac{y^2 + \beta_y^2 p_y^2}{2\sigma_y^2} \right). \quad (1.99)$$

Linearize the space charge force for small $|x|$ and $|y|$ to obtain

$$\vec{F} \approx \frac{2Q^2e^2\lambda}{\gamma^2} \left[\frac{x}{\sigma_x(\sigma_x + \sigma_y)} \hat{x} + \frac{y}{\sigma_y(\sigma_x + \sigma_y)} \hat{y} \right]. \quad (1.100)$$

Show that the envelope equation reads

$$\begin{aligned} \sigma_x'' + K_x\sigma_x - \frac{\epsilon_{x,\text{rms}}^2}{\sigma_x^3} &= \frac{\xi}{2(\sigma_x + \sigma_y)}, \\ \sigma_y'' + K_y\sigma_y - \frac{\epsilon_{y,\text{rms}}^2}{\sigma_y^3} &= \frac{\xi}{2(\sigma_x + \sigma_y)}. \end{aligned} \quad (1.101)$$

The nonlinear space charge force associated with a Gaussian beam will cause the distribution to deviate from being Gaussian, but this fact is ignored when writing Eq. (1.101).